The Ellipselet Transform

Abstract

Background: A fair amount of important objects in natural images have circular and elliptical shapes. For example, the nucleus of most of the biological cells is circular, and a number of parasites such as Oxyuris have elliptical shapes in microscopic images. Hence, atomic representations by two-dimensional (2D) basis functions based on circle and ellipse can be useful for processing these images. The first researches have been done in this domain by introducing circlet transform. **Methods:** The main goal of this article is expanding the circlet to a new one with elliptical basis functions. **Results:** In this article, we first introduce a new transform called ellipselet and then compare it with other X-let transforms including 2D-discrete wavelet transform, dual-tree complex wavelet, curvelet, contourlet, steerable pyramid, and circlet transform in the application of image denoising. **Conclusion:** Experimental results show that for noises under 30, the ellipselet is better than other geometrical X-lets in terms of Peak Signal to Noise Ratio, especially for Lena which contains more circular structures. However, for Barbara which has fine structures in its texture, it has worse results than dual-tree complex wavelet and steerable pyramid.

Keywords: *Basis functions, circlet, ellipselet, image denoising, X-lets*

Zahra Khodabandeh[1,2], Hossein Rabbani[1,3], Alireza Mehri Dehnavi[1,3], Omid Sarrafzadeh[4]

[1]Department of Bioelectrics and Biomedical Engineering, School of Advanced Technologies in Medicine, Isfahan University of Medical Sciences, [2]Student Research Committee, School of Advanced Technologies in Medicine, Isfahan University of Medical Sciences, [3]Medical Images and Signal Processing Research Center, School of Advanced Technologies in Medicine, Isfahan University of Medical Sciences, [4]Department of Biomedical Engineering, Mashhad Branch, Islamic Azad University, Mashhad, Iran

Introduction

In recent years, one of the most considerable approaches in image modeling is using transforms with different basis functions. For example, the atoms of discrete Fourier transform (DFT) are sine and cosine functions which can analyze the frequency component of stationary signals; however, they are not appropriate for analyzing nonstationary signals such as local visual properties in natural images (e.g., edge detection). Hence, although DFT has a high-frequency resolution, it suffers from lack of time/spatial resolution. In order to solve this weakness, the wavelet transform (WT) has been introduced for joint time–frequency analysis of signals.[1] This multiresolution transform is a powerful tool in signal/image analysis and has many applications in denoising, enhancement, and feature extraction. Indeed, DFT and WT are defined for one-dimensional (1D) signals, and they cannot efficiently represent geometries in natural images. In fact, these transforms can efficiently model the point-singularities, and even though they have many applications in signal processing tasks, they are not efficient enough for representing two-dimensional (2D)

singularities such as edges and curves in natural images. Note that extending 1D-discrete wavelet transform (DWT) to 2D-DWT does not solve this problem because 2D-separable DWT which is the tensor product of 1D-DWT reconstructs the 2D singularities by aggregation of point singularities around the edges which cannot model the smoothness along the direction of edges. In order to obviate the weaknesses of wavelets in larger dimensions, nonseparable 2D multiscale transforms called geometrical X-lets have been proposed. Ridgelet transform is one of these X-lets which was first introduced by Candes and Donho in 1999.[2] The ridgelet transform represents line singularity in 2D by using Radon transform and maps these singularities to point singularities. In addition to scale and translation parameters which are considered by DWT, the ridgelet transform also considers angle parameter. In addition, to represent the curve singularities in an image, the ridgelet transform has been extended to a new X-let called curvelet transform.[3] The curvelet transform is one of the multiscale transforms which provides analysis in some windows with different sizes to segment curves as a set of straights in subimages. The main idea behind this transform is decomposing an

Address for correspondence:
Dr. Alireza Mehri Dehnavi, Department of Bioelectrics and Biomedical Engineering, School of Advanced Technologies in Medicine, Isfahan University of Medical Sciences, Isfahan, Iran, Medical Images and Signal Processing Research Center, School of Advanced Technologies in Medicine, Isfahan University of Medical Sciences, Isfahan, Iran. E-mail: mehri@med.mui.ac.ir

image to multiresolution sub-bands and then analyzing each partitioned sub-band by ridgelet transform.[4] One of the main drawbacks of this transform is its need to discretization (e.g., rotating the curvelet basis functions can be easily performed in polar domain, but it is a challenging task in the Cartesian domain). To solve this problem, contourlet transform has been developed[5] which is directly defined in the discrete domain. The contourlet transform, at first, employs a multiscale transform to the images for detecting the edges, and then a local directional filter bank is applied for detecting contour segments.[6] In addition to lines and curves, circular and elliptical shapes are frequently seen in some medical images. For example, the nucleus of most of the biological cells is circular, and a number of parasites such as Leishmania and Oxyuris have elliptical shapes. Hence, introducing 2D basis functions based on circle and ellipse in atomic representations can be useful for processing these images. The first researches have been done in this domain by introducing circlet transform.[7] This transform decomposes an image using a set of circles with different radii and a determined width via a DFT filter bank. The main goal of this article is extending the theory of circlet transform to produce a new X-let transform with elliptical basis functions, i.e., ellipselet transform. In this article, first, the X-let transforms are explained briefly in X-let Transforms section. The Ellipselet Transform section is dedicated for introducing ellipselet transform by changing the circular basis functions to elliptical ones, and the results of ellipse detection using ellipselet transform on a simple image is explained in this section. For comparing the new transform with other X-lets, image denoising application with presented X-lets is compared in X-Lets for Image Denoising section. Finally, this article is discussed in Discussion and Conclusion section.

X-let Transforms

Usually, transforms decompose an image to a series of elementary waveforms called basis functions or dictionary atoms. Different directional time–frequency dictionaries provide various geometrical X-let transforms in two or higher dimensions. In this article, we provide a snapshot of a number of geometrical X-let transforms including 2D-DWT, dual-tree complex WT (DT-CWT), curvelet transform, contourlet transform and steerable pyramid, and circlet transform and introduce a new one namely ellipselet transform which is an extension of the circlet transform by modifying the circular basis function to the elliptical atoms.

Discrete wavelet transform

DWT is a powerful tool for joint time–frequency analysis of signals which decomposes a signal based on a series of basis functions called wavelets. The wavelets are produced by dilation and translation of a mother wavelet. This transform can show point singularities properly, but it is not an optimal tool for the representation of 2D singularities. For image processing, a simple way for using DWT is using tensor product for the extension of 1D-DWT to 2D-DWT. 2D-DWT provides a multiresolution representation by creating four sub-bands in each scale [Figure 1]. As shown in Figure 2, the basis functions of 2D-DWT can recognize vertical, horizontal, and diagonal spectral features. Although this transform has been used vastly in different applications of signal processing, it has some limitations such as lack of shift invariance and poor directional selectivity.[1]

Dual-tree complex wavelet transform

DT-CWT is one of the extensions of WT, which is first introduced by Kingsbury in 1998.[9] This transform uses two real DWTs in parallel as shown in Figure 3 to create real and imaginary parts of the transform. By producing six sub-bands in six directions, it has partly improved the deficiencies of 2D-DWT. In addition, the redundancy factor of this transform is 2^d for d-dimensions.[10] Figure 4 shows the sub-bands of DT-CWT in the direction of ±15, ±45, and ±75.

Discrete curvelet transform

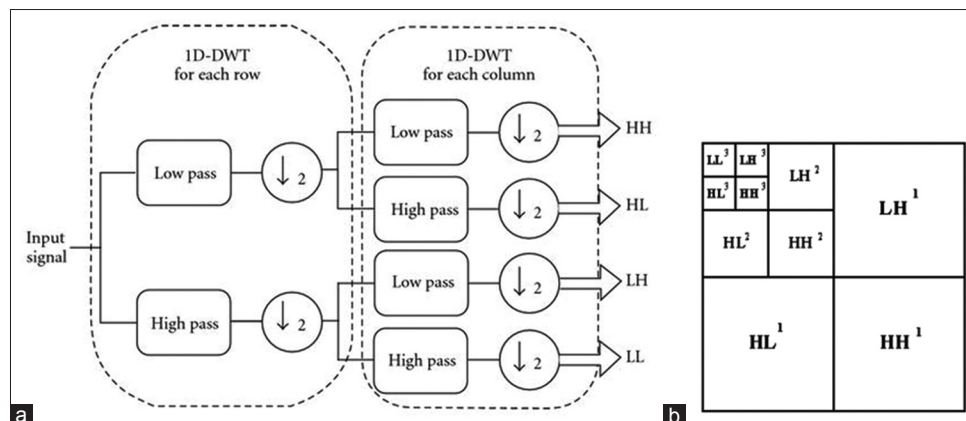The ridgelet transform, introduced by Cand'es and Donho,[2] is an efficient tool for representing line

Figure 1: (a) Filter structure of two-dimensional-discrete wavelet transform. (b) Two-dimensional-discrete wavelet transform decomposition in three levels[3]

singularities. Moreover, for demonstrating curves in images, this transform has been developed to curvelet transform. The curvelet is a multiscale transform which uses scaling, translating, and rotating parameters to create its basis functions. The main idea behind the curvelet transform is decomposing an image into sets of wavelet sub-bands and then analyzing each sub-band with the local ridgelet transform.[2] The block diagram of the first version of curvelet transform and its sub-bands are shown in Figures 5 and 6, respectively.

Discrete contourlet transform

The contourlet transform was first introduced by Do and Vetterli[5] to overcome the limitations of curvelet transform in discretization. This transform can detect 2D-geometrics in images in two steps: first, it decomposes an image into a set of sub-bands by Laplacian Pyramid and then applies a series of directional filter banks to
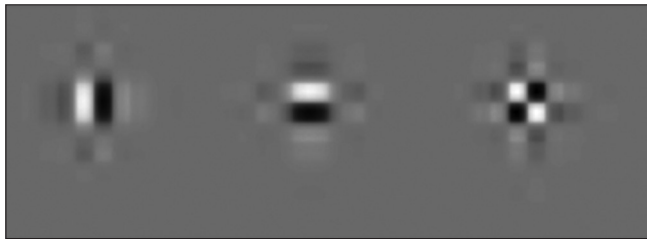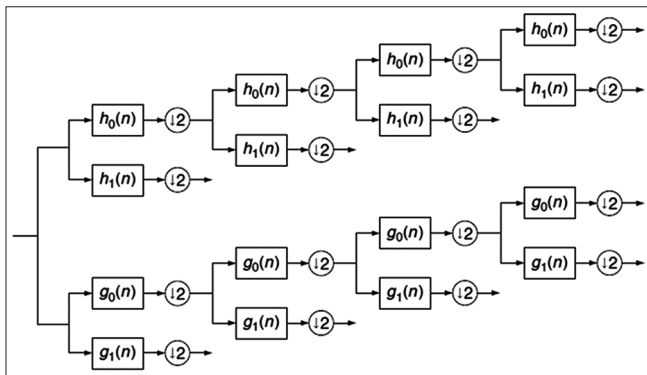
the image. The basis functions are oriented in different scales and orientations.[6] The block diagram of the Contourlet transform and its sub-bands are illustrated in Figures 7 and 8, respectively.

Steerable pyramids

The steerable pyramid is a linear multiscale and multiresolution transform based on angular and radial decompositions.[13] According to Figure 9, first, the image is divided into low- and high-pass sub-bands. Second, the low-pass sub-band is separated into a series of oriented band-pass sub-bands and a low-pass sub-band. Then, the low-pass sub-band is downsampled by a factor of 2, and this process will be repeated. If the transform has k orientation bands, it would be overcomplete by a factor of $4k/3$, showing redundancy.[14]

Circlet transform

The circlet transform is a robust tool to detect circular objects in images in which the binary image segmentation is not needed. The transform decomposes an image to a set of circles with different radii and a determined width using a DFT filter bank. This decomposition is defined in Fourier domain using the following definitions which are very close to the one introduced by Chauris *et al.*[7] The circlet parameters are described by a central position (x_0, y_0), radius (r_0), and central frequency content (f_0). All circlet components $C_\mu (x, y)$ can be obtained by a reference circlet $C_{ref} (x, y)$ which can be shifted or changed in radius and central frequency content of the circlet. The circlet function is defined by the following equation:

$$C_\mu (x, y) = \Omega \left[2\pi f_0 \left(r - r_0 \right) \right] \qquad (1)$$

Where, $r = \sqrt{\left(x - x_0 \right)^2 + \left(y - y_0 \right)^2}$ and Ω is an oscillating function such as wavelet function to distinguish discontinuities. Practically, C_μ is defined in 2D Fourier domain.[7] In circlet decomposition, an image $f(x, y)$ is broken down into a sum of basic functions C_μ as shown in Eq. 2:

$$f (x, y) = \sum_\mu A_\mu C_\mu (x, y) \qquad (2)$$

Figure 2: Sub-bands of two-dimensional-discrete wavelet transform[8]

Figure 3: Analysis of filter bank for the dual-tree complex discrete wavelet transform[10]
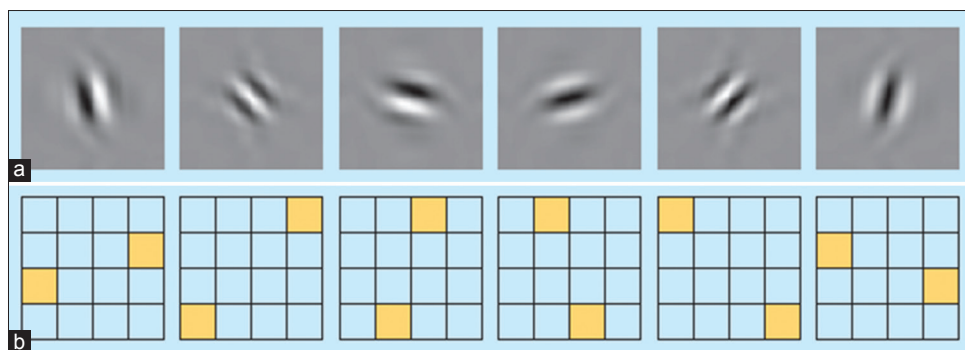

Figure 4: The sub-bands of real oriented two-dimensional dual-tree complex discrete wavelet transform in (a) space domain (b) Fourier spectrum[10]

The circlet transform is a tight frame system, and the amplitudes A_μ are created by a scalar product as shown in Eq. 3:

$$A_\mu = <f, C\mu> = \iint f(x,y) \, C\mu(x,y) \, dx \, dy \qquad (3)$$

From a practical point of view, the circlet coefficients can be defined in the Fourier domain using Parseval's theorem as shown below:

$$A_\mu = <\hat{f}, \hat{C}\mu> = \iint \hat{f}(\omega_1, \omega_2) \hat{C}\mu^n(\omega_1, \omega_2) \, d\omega_1 \, d\omega_2 \qquad (4)$$

Where $\hat{f}$ is the 2D Fourier transform of f and f^* is the conjugate of f. Hence, the circlet transform is defined in 2D Fourier domain with the definition of; $\hat{C}\mu(\omega_1, \omega_2)$, the Fourier transform of $C\mu$ plays an important role in the performance of circlet transform.

In order to construct circular-shaped filters, 1D filters F_k and 2D filters G_k are used such that for all ω and (ω_1, ω_2), the following perfect reconstruction conditions are satisfied:

$$\sum_k |F_k(\omega)|^2 = 1$$
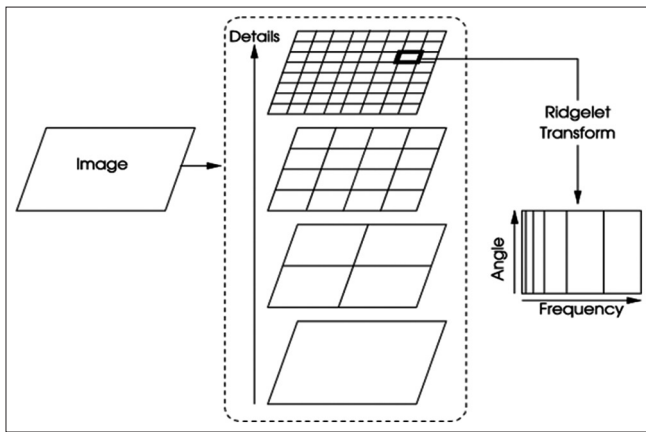
$$\sum_k |G_k(\omega_1, \omega_2)|^2 = 1 \qquad (5)$$

Figure 5: The block diagram of curvelet transform[11]

In these conditions, the filter F_k is defined as shown in Eq. 6, where N is the number of filters and

$$\omega_k = \frac{\pi(k-1)}{N-1}$$

$$F_k = \begin{cases} \cos(\omega \pm \omega_k), & |\omega \pm \omega_k| <= \dfrac{\pi}{N-1} \\ 0, & other \end{cases} \qquad (6)$$

In order to construct circular shape in spatial domain, the 2D filter G_k is defined by a phase delay of 1D filter as F_k shown in Eq. 7.

$$G_k(\omega_1, \omega_2) = e^{j|\omega|r_0} . F_k(|\omega|) \qquad (7)$$

In Eq. 7, $\omega(\omega_1, \omega_2) = |\omega|$ and is defined as follows:

$$|\omega| = \sqrt{\omega_1^2 + \omega_2^2} \qquad (8)$$

By the definition of G_k, the Fourier transform of a circlet is described in Eq. 9.

$$\hat{G}_\mu = e^{i<\omega.xc>} . G_k(\omega) \qquad (9)$$

Where $x_c = (x0, y0)$ is the central position, and r_0 is the radius of the circlet. Figure 10 shows the magnitude and phase of basis functions in circlet transform.[16]

Ellipselet Transform

The main goal of this study is expanding the circlet transform to a new one with elliptical basis functions. Therefore, we have to design a new atomic representation system with elliptical basis functions. As mentioned in Eq. 7, in $F_k|\omega|$ and for $\omega = (\omega_1, \omega_2)$, $|\omega|$ is defined by the Eq. 8 that it constructs the circular shape of basis functions in circlet. Now, we introduce a new norm definition as follows:

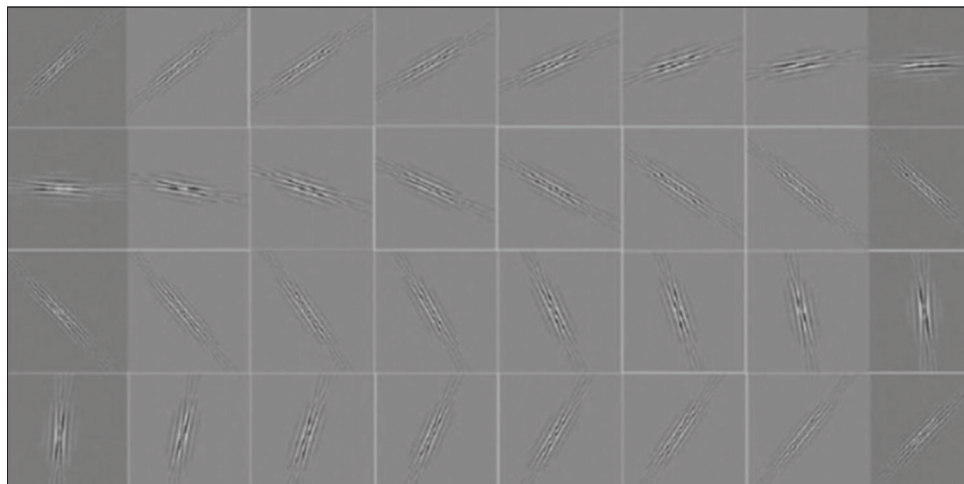$$|\omega|_{elp} = \sqrt{k_1\omega_1^2 + k_2\omega_2^2 + \alpha\omega_1\omega_2} \qquad (10)$$

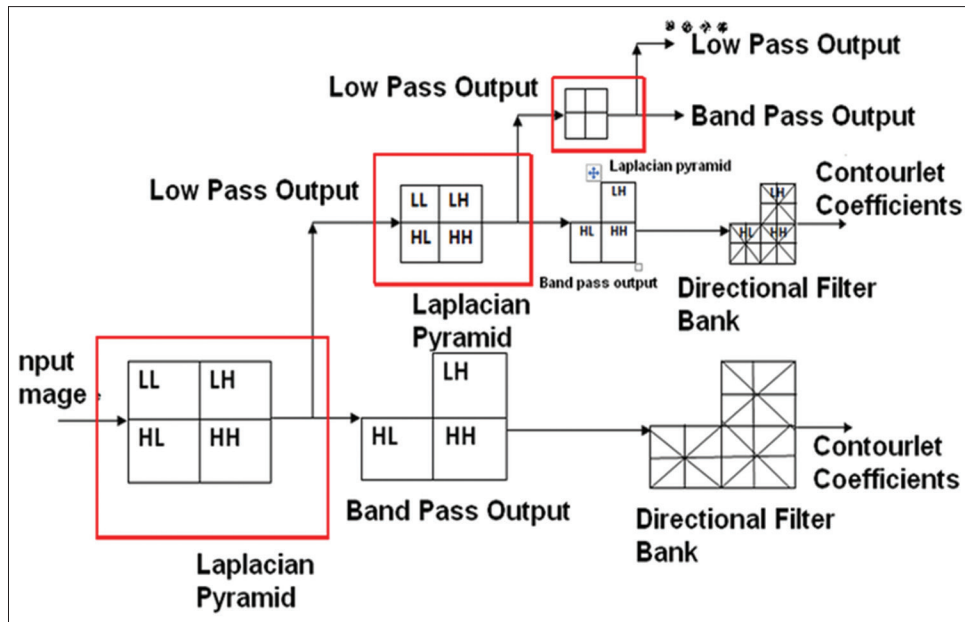
Figure 6: Sub-bands of curvelets[8]

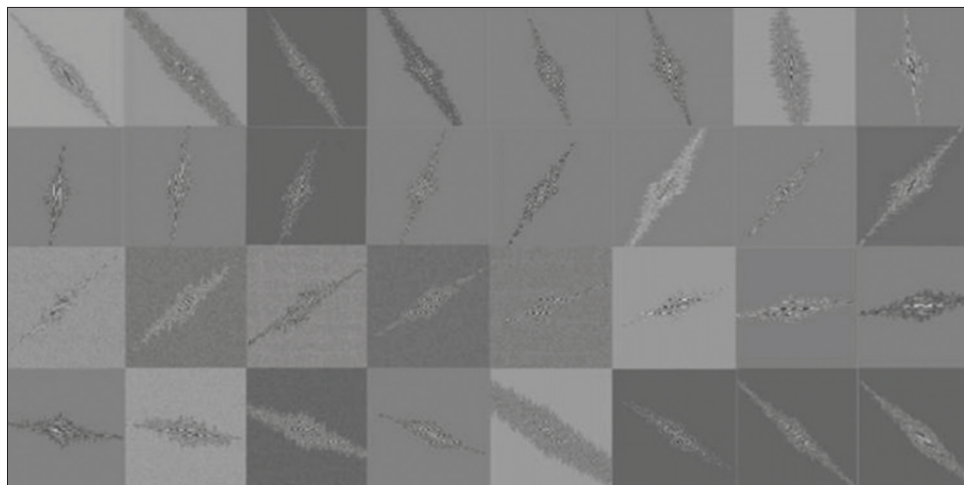**Figure 7: The block diagram of contourlet transform[12]**

Figure 8: Sub-bands of contourlet[8]

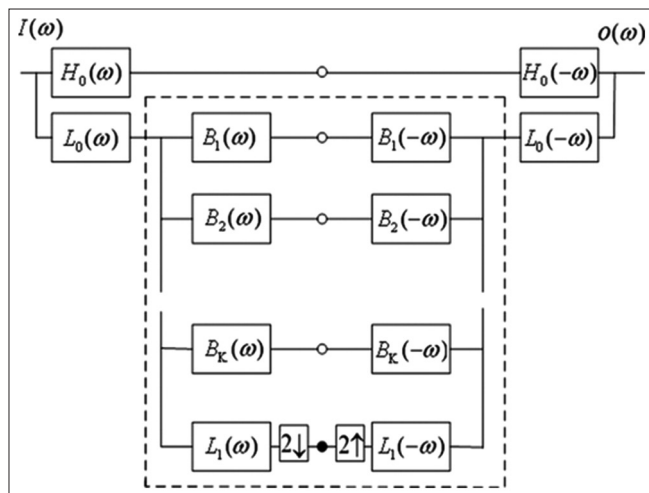**Figure 9: The block diagram of steerable pyramid decomposition[15]**

In this equation, by considering different values of k_1 and k_2 and α parameters, elliptical basis functions in different sizes and directions are built. We assume that we have a new transform with four basis functions in four different directions as shown in Figure 11.

For detecting ellipses in images, we need to know the position, angle, and size of the major and minor axes of ellipse. We assume a simple ellipse as shown in Figure 12.

The produced sub-bands of Figure 12 using the introduced basis functions in Figure 11 are represented in Figure 13. As shown, the first row which is related to basis functions at 0° is similar to the original image. By converting the sub-bands to binary images and using morphological operations, the new subimages as shown in Figure 14 are achieved.
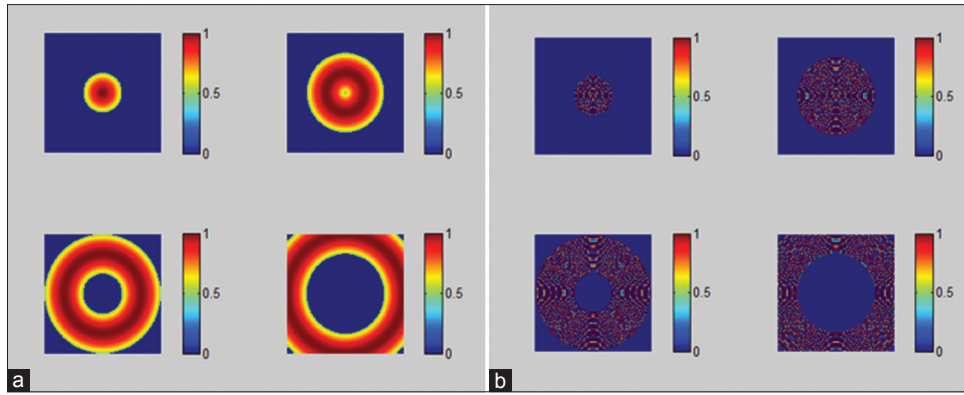
Figure 10: (a) The magnitude of basis functions of circlet transform. (b) The phase of basis functions of circlet transform
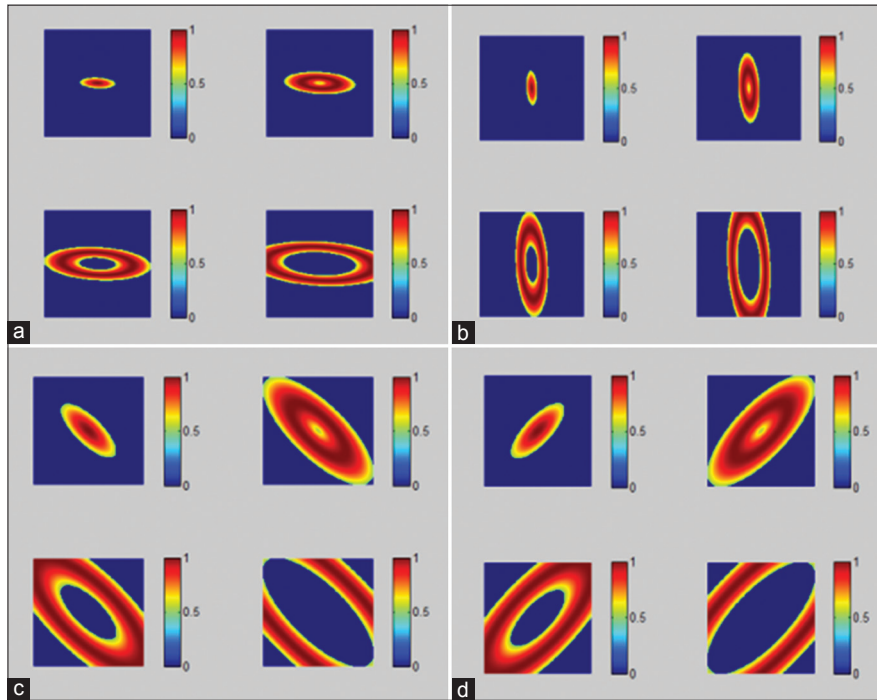

Figure 11: Basis functions of the ellipselet transform in four directions and four frequency contents. (a-d) the basis function at angles 0°, 90°, −45°, and 45°, respectively
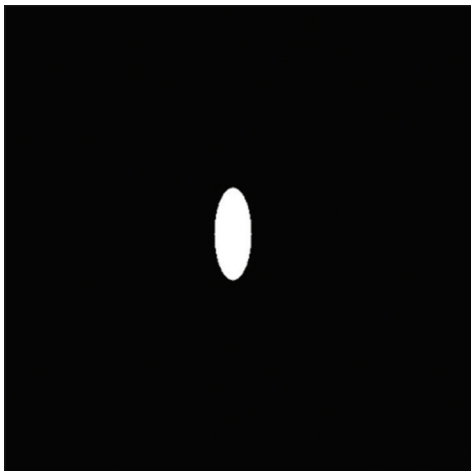

Figure 12: A simple ellipse with major axis: 50 pixels, minor axis: 20 pixels, angle: 90, center position: (250, 250), size of image: (512, 512)

It is obvious from Figure 14 that only sub-bands in the first row are similar to the original image which is related to the basis functions with zero direction. In order to find the desired size and location of the ellipse, radon transform can be employed.[17] If we use radon transform for each sub-band in the angle of perpendicular direction of its basis, we achieve signals as shown in Figure 15. We consider a percentage of maximum of peaks in signals for thresholding of signals as shown in Figure 15. By choosing the sub-band in which all the four sub-images are above the threshold, the first sub-band is extracted that is related to the basis of zero direction and shows that the main ellipse is in vertical direction at 90°. Now, for detecting the position of the main ellipse, all row/column signals of the selected sub-band are plotted and the middle of two
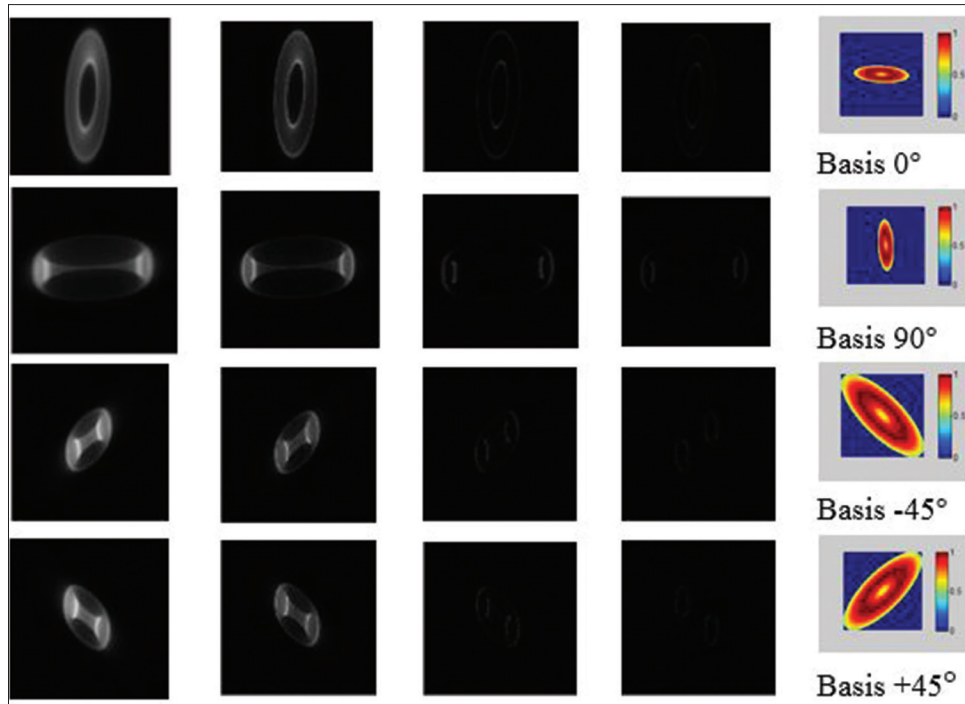
Figure 13: The sub-bands of ellipselet transform on the ellipse of Figure 12
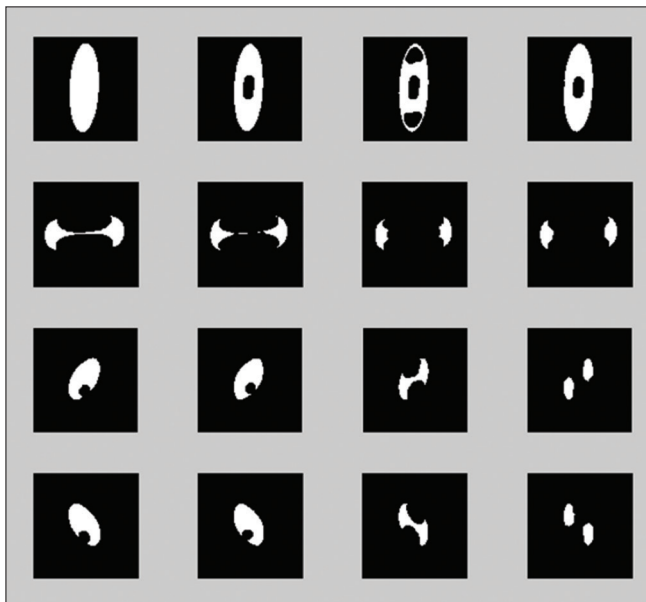

Figure 14: Produced subimages of Figure 13 after binerization and applying morphological operators

maximum points is selected as the x/y position of the center of the desired ellipse [Figure 16].

After determining the center position and angle of the ellipse, we calculate the dimensions of the ellipse by using two radon transforms in the direction of the ellipse and its perpendicular line. Considering the obtained parameters of ellipse, we can draw the extracted ellipse by ellipselet transform. Figure 17 shows the contour of the produced ellipse in blue color. This figure shows that the position and angle of the ellipse have been detected correctly.

X-Lets for Image Denoising

In general, digital images suffer from noise due to acquisition/transmission process and shortcoming of capturing modalities and receivers. In addition to linear methods such as Wiener filtering, nonlinear techniques including applying thresholding/shrinkage functions in transform domains have been reported in recent years.[3,5,9,18,19] In general, in image transform-based denoising approaches, two important issues should be considered. The first one is choosing proper transform and the other is selecting proper thresholding function. In this article by using a proper thresholding function, the performance of geometrical X-lets such as 2D-DWT, DT-CWT, curvelet, contourlet, steerable pyramid, circlet transform, and the proposed transform of ellipselet was compared in reducing additive white Gaussian noise from natural images.

Experimental Results

Different frameworks can be considered for image denoising. Usually, reported studies in Bayesian frameworks outperform others. For example, Rabbani in 2009[19] used local Laplace pdf and maximum a posteriori (MAP) estimator in steerable pyramid domain and showed better performance in comparison with the other state-of-the-art denoising methods such as Bayes least squared Gaussian scale mixture technique.[20] The statistical features of images can be simplified in sparse domains because of some properties of transforms such as sparsity. Hence, the main features of transformed image can be represented by a few large coefficients, and the remained
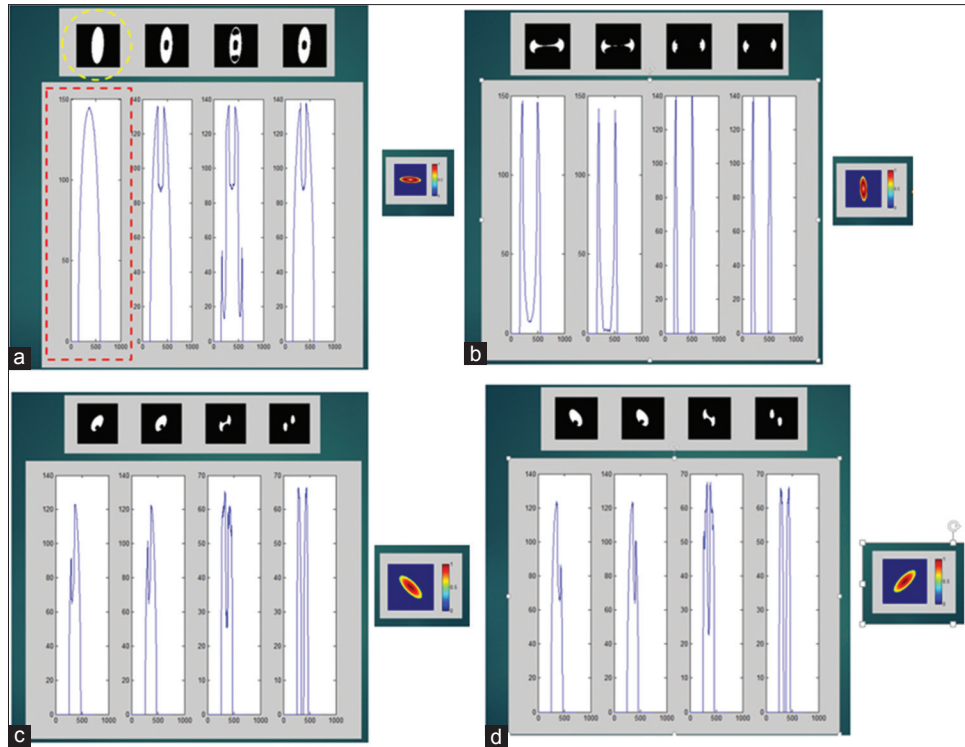
Figure 15: (a) Radon transform of the first row of Figure 14 in the direction of 90°. (b) Radon transform of the second row of Figure 14 in the direction of 0°. (c) Radon transform of the third row of Figure 14 in the direction of +45°. (d). Radon transform of the fourth row of Figure 14 in the direction of −45°
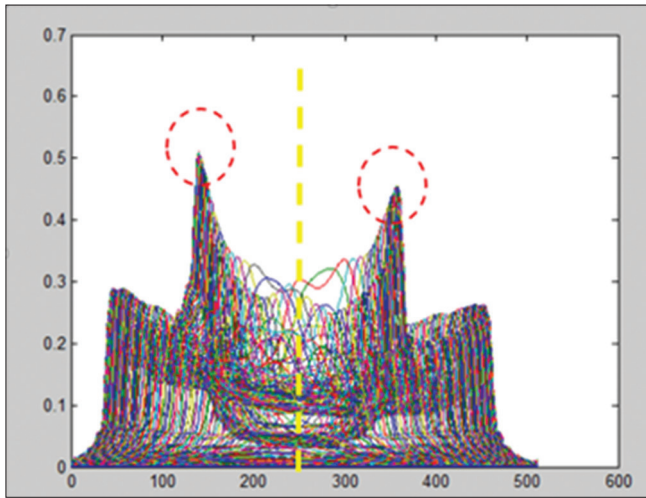

Figure 16: Selection of center of the desired ellipse
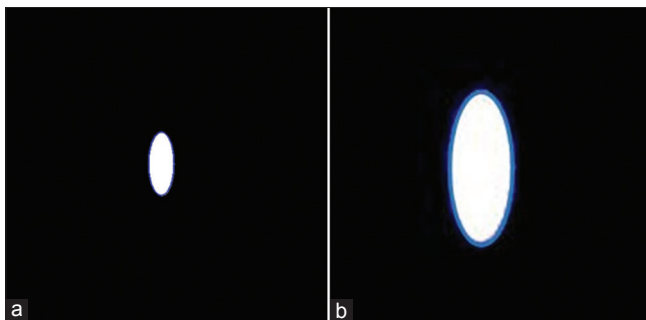

Figure 17: (a) Detected ellipse with the new transform. (b) The zoomed-in detected ellipse of part

coefficients are approximately around zero. Hence, there is a large peak at zero in the histogram of sub-bands and its tails goes to zero slower. It means that their distribution is close to the Laplace pdf and far from the Gaussian pdf. In this study, we first show the histogram of the X-let coefficients in a specific sub-band and then the Laplacian and Gaussian pdfs are fitted to the histogram [Figure 18], and the goodness of fit of each pdf is reported. Because Laplacian pdf is well fitted to the histograms, using MAP estimator and Laplacian prior, the soft thresholding with a threshold of $\sqrt{2}\dfrac{\sigma_n^2}{\sigma_k}$ is obtained,[19] where σ_n is the standard deviation of noise and σ_k is the standard deviation of noise-free image in the kth sub-band. Experiments performed on standard gray scale images of Lena, Barbara, and Boat at a resolution of 512×512 pixels corrupted by additive Gaussian noise with different levels to compare the performance of geometrical X-lets transforms in image denoising.

According to Figure 19, by testing different combinations of ellipselet sub-bands (for $n = 4$ in Eq. 6), the best signal-to-noise ratio is obtained on the first, third, and fourth sub-bands of ellipselet ([1,3,4]). Hence, for denoising by circlet and ellipselet transforms, the second sub-band, which includes the main global information of the image, remains unchanged, and soft thresholding is applied on the first, third, and fourth sub-bands. However, similar to the usual procedure of transform-based denoising methods for
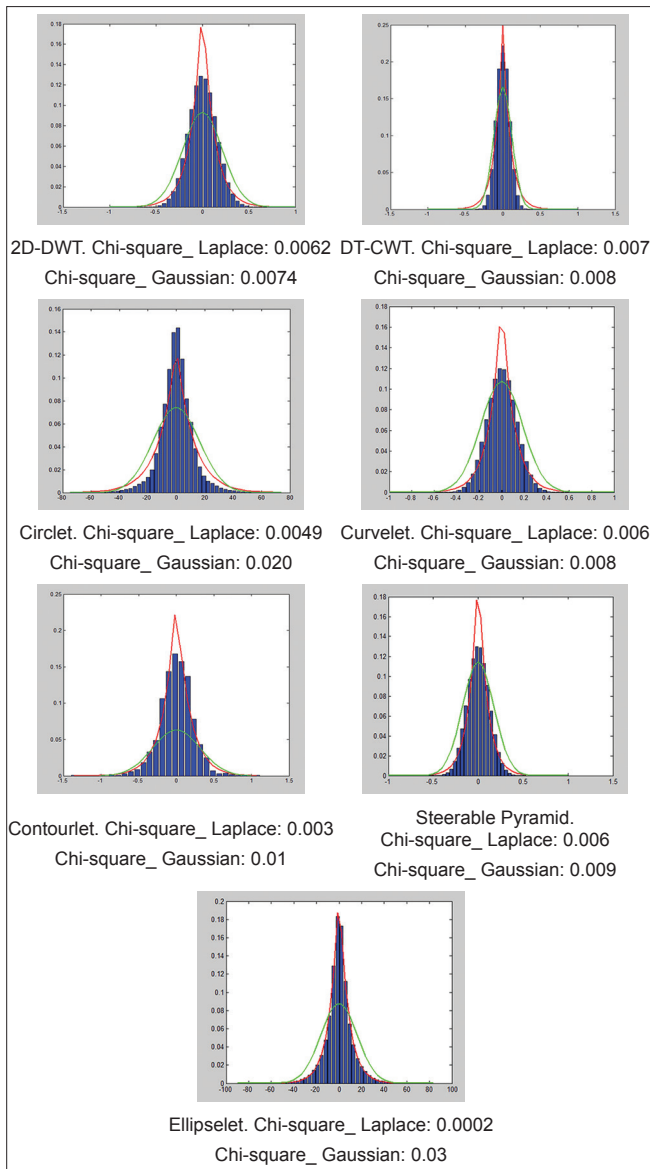
Figure 18: The histogram of the X-Let coefficients in a specific sub-band of Lena image and the best Gaussian (green plot) and Laplace pdf (red plot) fitted to this histogram with Chi-square test

other X-lets, in this article, the low-pass sub-band is kept unchanged and the thresholding function is applied on other sub-bands.

The efficiency of the presented methods is first visually evaluated as shown in Figures 20 and 21. Then, the experimental results are numerically compared in terms of peak signal-to-noise ratio (PSNR) [Figure 22] and Structural Similarity Index (SSIM) [Table 1] using the following definitions:

$$PSNR = 10\log_{10}\left(\frac{MAX_i^2}{MSE}\right) \tag{11}$$

Where *MSE* is the mean squared error and MAX_t is the maximum possible pixel value of the image.

The SSIM shows structural similarities between two images and defines as follows.[21]

$$SSIM = \frac{\left(2\overline{s}\,\overline{\hat{s}}+2.55\right)\left(2\sigma_{s\hat{s}}+7.65\right)}{\left(\overline{s}^2+\overline{\hat{s}}^2+2.55\right)\left(\sigma_s^2+\sigma_{\hat{s}}^2+7.65\right)} \tag{12}$$

Discussion

In this article, we introduced a new X-let transform namely ellipselet transform by using elliptical basis functions. We showed that this transform can correctly detect a simple ellipse at 90°. For ellipses in three other directions of 0°, −45°, and +45°, we also did the same work described above and achieved the desired answers. Hence, the new transform with elliptical basis functions introduced in this article can detect the direction and position of simple ellipses in images. However, this new transform has some limitations. For example, it has limited number of basis functions, and we just tested it on simple images with one ellipse. Considering new criterions and expanding this transform by using more basis functions (e.g., 8 basis functions in angles 0°, ±22.5°, ±45°, ±67.5°, and 90°) is suggested in future studies.
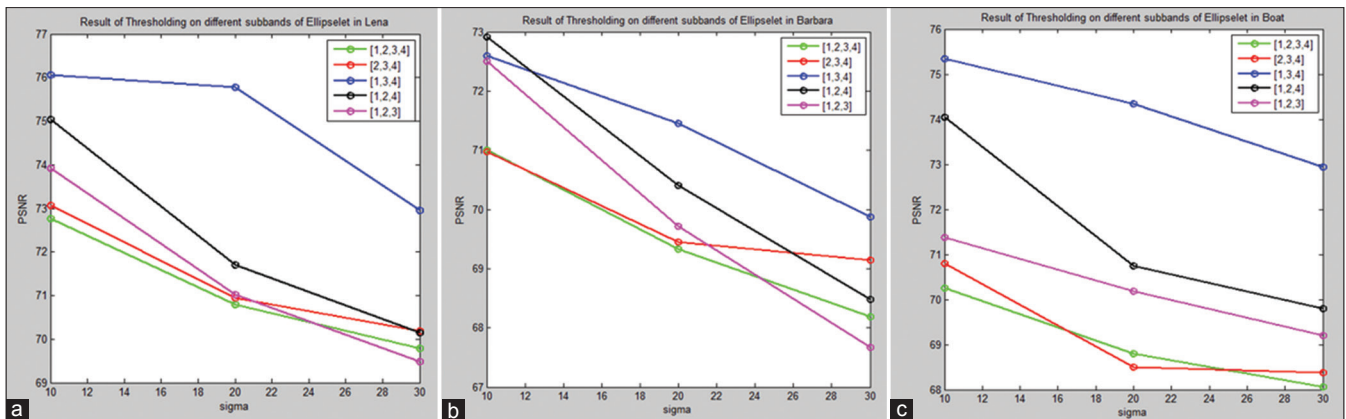

Figure 19: Comparison among thresholding on different sub-bands of ellipselet. (a) Peak signal-to-noise ratio of denoized Lena in different sub-band thresholding. (b) Peak signal-to-noise ratio of denoized Barbara in different sub-band thresholding. (c) Peak signal-to-noise ratio of denoized boat in different sub-band thresholding
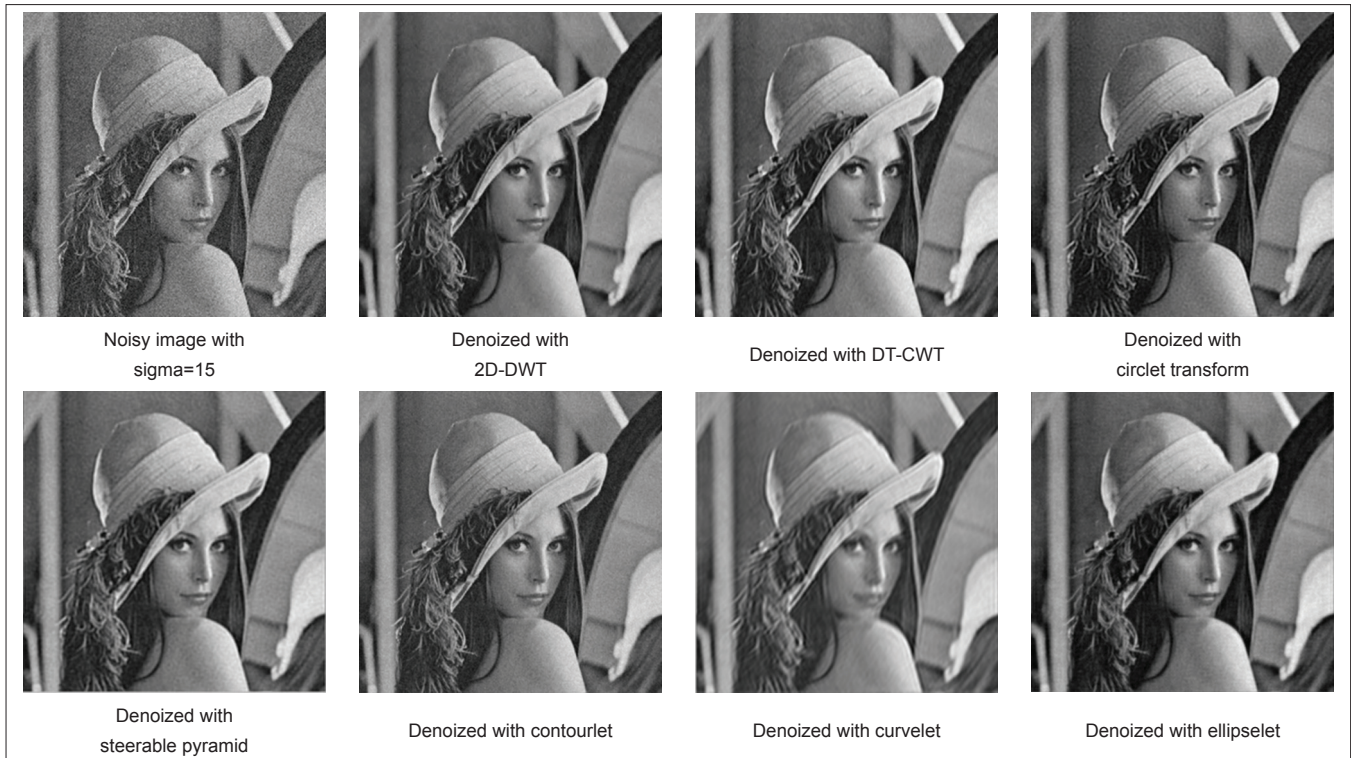
Figure 20: Results of image denoising of Lena with different X-lets for sigma = 15
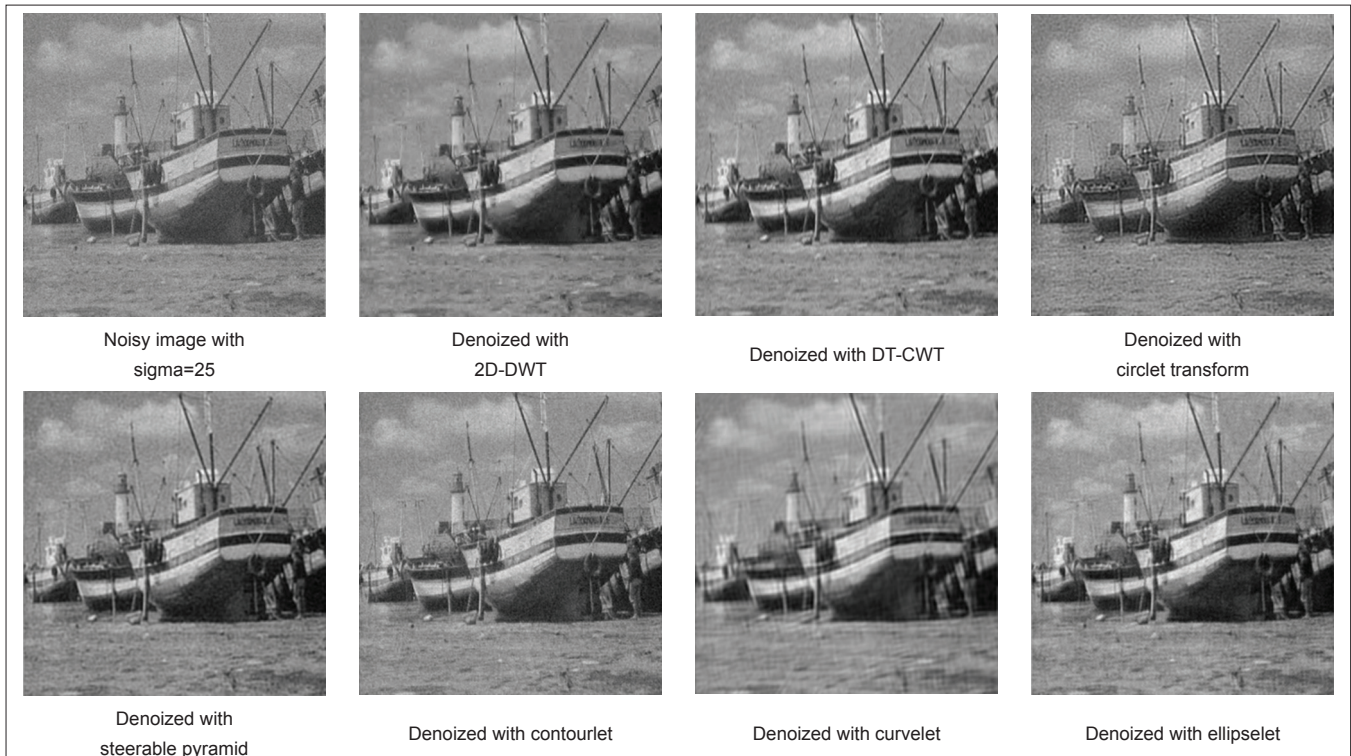
Figure 21: Results of image denoising of boat with different X-lets for sigma = 25

In this article, we also compared the introduced ellipselet transform with other X-let transforms in reducing noise from natural images. As shown in Figure 22, DT-CWT usually outperforms others in terms of PSNR. The main reason is that the DT-CWT has a good directional selectivity and perfect reconstruction property which makes it a proper tool for denoising applications. According to Table 1, DT-CWT has the maximum

SSIM for Boat and Barbara, and steerable pyramid has the maximum SSIM for Lena in different levels of noise. The reason of good performance of steerable pyramid is that the steerable pyramid operates based on a polar-separable decomposition in the frequency domain that allows independent representation of scale and orientation, and the representation is translation and rotation invariant which makes it proper to analyze image structures and edge preservation. Moreover, as shown in Figure 22, for noises under 30, the ellipselet is better than others, especially for Lena which contains more circular structures. However, for Barbara which has fine structures in its texture, it has worse results than DT-CWT and steerable pyramid.

Different results in different images by different levels of noise show that X-lets' performance is related to the image content and level of noise. As illustrated in Figure 23, the basis functions of different X-lets produce different frequency features, and each of them partitions the 2D frequency plane in a different way. Based on the location of components of image in 2D frequency plane and how they match with basis functions, any of these transforms could be more

Table 1: The results of structural similarity index for different denoising methods

512×512 image	σ	Noisy image	2D-DWT	DT-CWT	Circlet	Curvelet	Cotourlet	Steerable pyramid	Ellipselet
Lena	10	0.64	0.83	0.87	0.79	0.82	0.85	0.88	0.84
	15	0.50	0.79	0.82	0.71	0.78	0.78	0.82	0.79
	25	0.35	0.73	0.76	0.57	0.71	0.69	0.77	0.67
	35	0.28	0.68	0.73	0.47	0.67	0.64	0.75	0.56
	45	0.22	0.57	0.65	0.39	0.57	0.59	0.71	0.46
	55	0.19	0.54	0.63	0.31	0.53	0.55	0.68	0.39
	70	0.16	0.42	0.65	0.21	0.46	0.49	0.61	0.25
Boat	10	0.71	0.83	0.84	0.77	0.75	0.78	0.78	0.78
	15	0.58	0.78	0.78	0.71	0.70	0.68	0.74	0.74
	25	0.42	0.70	0.70	0.60	0.63	0.54	0.68	0.65
	35	0.33	0.63	0.64	0.50	0.56	0.47	0.62	0.57
	45	0.27	0.60	0.61	0.42	0.52	0.39	0.57	0.49
	55	0.24	0.58	0.59	0.35	0.51	0.34	0.52	0.43
	70	0.19	0.53	0.54	0.28	0.49	0.28	0.46	0.35
Barbara	10	0.72	0.83	0.84	0.67	0.72	0.76	0.69	0.74
	15	0.60	0.76	0.78	0.60	0.57	0.67	0.62	0.70
	25	0.45	0.68	0.69	0.50	0.55	0.54	0.59	0.61
	35	0.36	0.59	0.62	0.41	0.53	0.45	0.53	0.53
	45	0.30	0.56	0.57	0.36	0.50	0.39	0.49	0.45
	55	0.25	0.54	0.54	0.30	0.49	0.34	0.44	0.40
	70	0.22	0.50	0.52	0.24	0.47	0.27	0.39	0.33

2D-DWT – Two-dimensional discrete wavelet transform; DT-CWT – Dual-tree complex wavelet transform
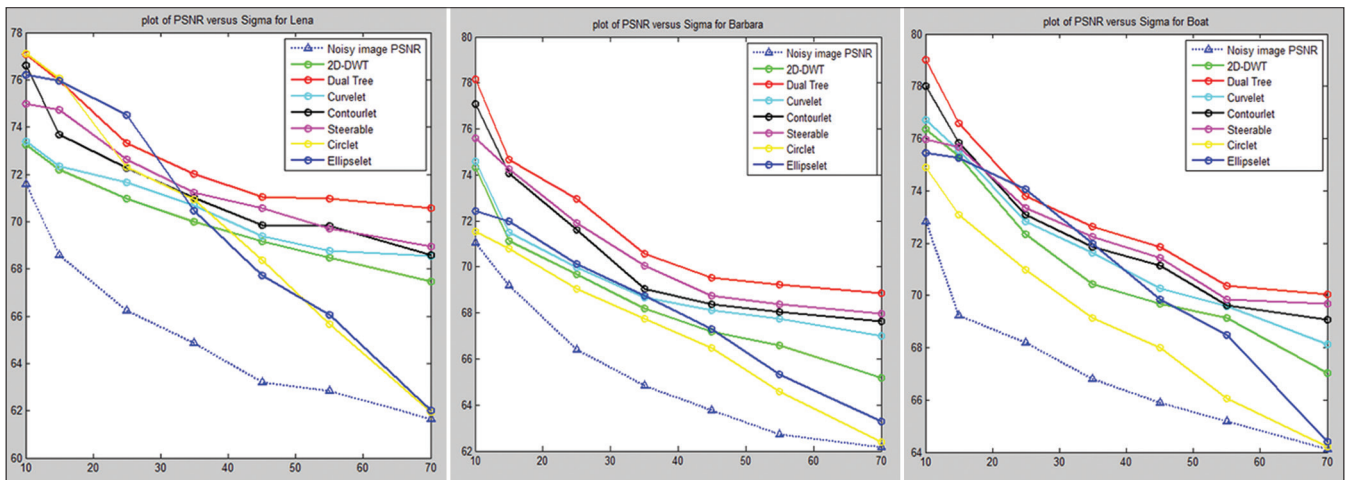

Figure 22: The results of peak signal-to-noise ratio for Lena and Barbara images denoised by different X-lets
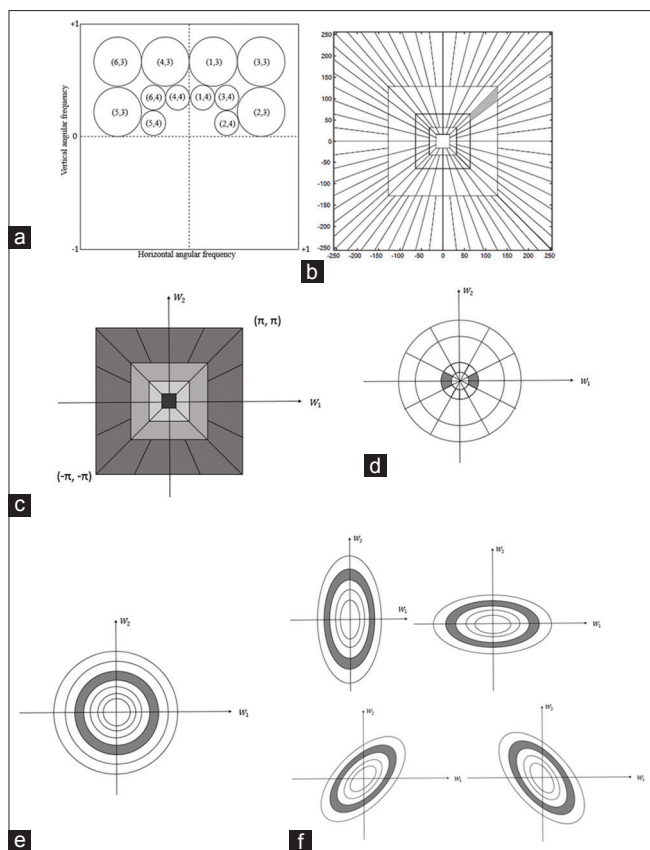
Figure 23: Frequency partitioning of: (a) Dual-tree complex wavelet, (b) curvelet,[22] (c) contourlet, (d) steerable pyramid, (e) circlet, (f) ellipselet in the directions of 0, 90, +45, −45

beneficial. About the newly introduced transform, ellipselet, we can see that it has better results than circlet transform and both of them have good results in lower levels of noise, especially for images containing circular patterns.

Financial support and sponsorship

None.

Conflicts of interest

There are no conflicts of interest.

References

1. Daubechies I, Bates BJ. Ten Lectures on Wavelets. J Acoust Soc Am 1993;93:1671.
2. Candes EJ, Donoho DL. Ridgelets: A key to higher-dimensional intermittency? Philos Trans R Soc A Math Phys Eng Sci 1999;357:2495-509.
3. Alzubi S, Islam N, Abbod M. Multiresolution analysis using wavelet, ridgelet, and curvelet transforms for medical image segmentation. Int J Biomed Imaging 2011;2011:136034.
4. Starck JL, Candès EJ, Donoho DL. The curvelet transform for image denoising. IEEE Trans Image Process 2002;11:670-84.
5. Do MN, Vetterli M. The contourlet transform: An efficient directional multiresolution image representation. IEEE Trans Image Process 2005;14:2091-106.
6. Yang L, Guo BL, Ni W. Multimodality medical image fusion based on multiscale geometric analysis of contourlet transform. Neurocomputing 2008;72:203-11.
7. Chauris H, Karoui I, Garreau P, Wackernagel H, Craneguy P, Bertino L. The circlet transform: A robust tool for detecting features with circular shapes. Comput Geosci 2011;37:331-42.
8. Amini Z, Rabbani H. Classification of medical image modeling methods: A review. Curr Med Imaging Rev 2016;12:1. [Last cited on 2019 May 20].
9. Kingsbury N. The Dual-Tree Complex Wavelet Transform: A New Efficient Tool for Image Restoration and Enhancement; 1998.
10. Selesnick IW, Baraniuk RG, Kingsbury NC. The dual-tree complex wavelet transform. IEEE Signal Process Mag 2005;22:123-51.
11. Lambert P, Pires S, Ballot J, García RA, Starck JL, Turck-Chièze S. Curvelet analysis of asteroseismic data I: Method description and application to simulated sun-like stars. Astron Astrophys 2006;454:1021-7.
12. Satheesh S, Prasad K. Medical image denoising using adaptive threshold based on contourlet transform. Adv Comput Int J 2011;2:52-8.
13. Simoncelli EP, Freeman WT. The steerable pyramid: A flexible architecture for multi-scale derivative computation. In: Proceedings, International Conference on Image Processing. Washington,DC. IEEE Comput Soc Press; 1995. p. 444-7.
14. Simoncelli EP, Freeman WT, Adelson EH, Heeger DJ. Shiftable multiscale transforms. IEEE Trans Inf Theory 1992;38:587-607.
15. Wang J. Exposure fusion based on steerable pyramid for displaying high dynamic range scenes. Opt Eng 2009;48:117003.
16. Sarrafzadeh O, Dehnavi AM, Rabbani H, Ghane N, Talebi A. Circlet based framework for red blood cells segmentation and counting. In: 2015 IEEE Workshop on Signal Processing Systems (SiPS). IEEE; 2015. p. 1-6.
17. Comaniciu D, Meer P. Mean shift: A robust approach toward feature space analysis. IEEE Trans Pattern Anal Mach Intell 2002;24:603-19.
18. Hamdi M. A comparative study in wavelets, curvelets and contourlets as denoising biomedical Images. Image Process Commun 2011;16:13-20.
19. Rabbani H. Image denoising in steerable pyramid domain based on a local Laplace prior. Pattern Recognit 2009;42:2181-93.
20. Portilla J, Strela V, Wainwright MJ, Simoncelli EP. Image denoising using scale mixtures of Gaussians in the wavelet domain. IEEE Trans Image Process 2003;12:1338-51.
21. Wang Z, Bovik AC, Sheikh HR, Simoncelli EP. Image quality assessment: From error visibility to structural similarity. IEEE Trans Image Process 2004;13:600-12.
22. Candès E, Demanet L, Donoho D, Ying L. Fast discrete curvelet transforms. Multiscale Model Simul 2006;5:861-99.

BIOGRAPHIES

Zahra Khodabandeh is a PhD candidate at Isfahan University of Medical Sciences. She received her BSc and MSc degree in biomedical engineering from Isfahan University and Isfahan University of Medical Sciences, Isfahan, Iran in 2011 and 2017, respectively. Her current research interests include medical image analysis, machine learning and deep learning.

Email: shimakhodabandeh@yahoo.com

Hossein Rabbani received his BSc degree in electrical engineering from Isfahan University of Technology, Isfahan, Iran, in 2000, and his MSc and PhD degrees in bioelectrical engineering from Amirkabir University of Technology, Tehran, Iran, in 2002 and 2008, respectively. He is now a full professor in the Biomedical Engineering Department, Isfahan University of Medical Sciences, Isfahan. His research interests are medical image analysis and modeling, signal processing, sparse transforms, and image restoration.

Email: h_rabbani@med.mui.ac.ir

Alireza Mehri Dehnavi received his BSc degree in electronic engineering from Isfahan University of Technology in 1988. He received his MSc degree in measurement and instrumentation from Indian Institute of Technology Roorkee, India, in 1992 and his PhD in medical engineering from Liverpool University in 1996. He is a full professor in the Biomedical Engineering Department, Isfahan University of Medical Sciences, Isfahan, Iran. His research interests are medical optics, devices and signal, and image processing.

Email: mehri@med.mui.ac.ir

Omid Sarrafzadeh received his PhD in biomedical engineering from Isfahan University of Medical Sciences, Isfahan, Iran. He is assistant professor in Islamic Azad University Mashhad Branch. His research interests are image and signal processing and pattern recognition.

Email: o.sarrafzade@gmail.com